Cadmium Ion Adsorption on Carboxyl-Terminated Iron Oxide Beads

Jun Wu, Josephine Sun, Ionel C. Stefan, and Daniel A. Scherson*

Department of Chemistry, Case Western Reserve University, Cleveland, Ohio 44106-7078

Received: June 17, 2004

The affinity of Cd^{2+} toward carboxyl-terminated iron oxide beads (C-TIOB, Sigma) suspended in aqueous solutions was investigated using anodic stripping voltammetry (ASV) as a function of both pH and [Cd^{2+}] in the μM range. Advantage was taken of the superparamagnetic character of C-TIOB to confine and/or remove the beads *within* the enclosed vessel, using an external magnet, and thus assess the influence of dispersed C-TIOB on the amount of Cd^{2+} detected by ASV. Within experimental error, the difference between ASV data recorded before and after adding and then confining the particles by magnetic means, which provides a measure of the amount of Cd^{2+} adsorbed on C-TIOB, was found to yield results comparable to those of identical measurements with fully dispersed C-TIOB. Adsorption data collected as a function of [Cd^{2+}] and pH revealed a marked increase in the binding constant of Cd^{2+} for carboxylate ions upon attachment to the solid support, over values predicted strictly from standard solution phase equilibria.

Introduction

The binding of metal ions in solution to macromolecules and solid surfaces is of pivotal interest to a variety of disciplines ranging from biology to geology.[1−3] Such interactions involve, by and large, functional groups, as in the case of proteins,[1,4,5] or specific surface sites, as in metal oxides and oxyhydroxides, particularly of iron and aluminum.[6,7] Attention has been focused in our laboratory on the implementation of attenuated total reflection-Fourier transform infrared (ATR-FTIR) for the spectroscopic detection of metal-ion binding to self-assembled monolayers (SAMs) incorporating alkane chains bearing carboxylic/carboxylate[8,9] or pyridyl terminal groups.[10] For those studies, SAMs were formed spontaneously on the surface of a second alkane chain SAM exposing methyl terminal moieties at one end and covalently linked to the surface of a Ge internal reflection element (IRE) through siloxane groups at the other.[8,9] Much of the effort has centered on the interactions of Cd^{2+} with such biomimetic analogues of cell membranes motivated in part by the adverse effects of this highly toxic metal ion on the nervous system, lungs, testis, pancreas, and placenta in humans. Increases in the concentration of Cd^{2+} in the body have been traced primarily to cigarette smoking, ingestion of contaminated food, especially fish and grain and cereal products, and also occupational hazards, such as those derived from battery, metal coating and alloy industries.[1]

The degree of environmental toxicity of Cd^{2+} and that of other heavy metal ions as well is controlled by the thermodynamics and kinetics of adsorption on soil components, especially humic and fulvic acids, and hematite. In fact, the use of phosphatic fertilizers, and the settling of air borne industrial pollution have led to alarming increases in the amount of Cd^{2+} in certain agricultural land areas.[3] Among the research strategies being pursued to assess the degree of contamination are direct measurements on actual soil using ex situ ICP-AE for Cd-content determination.[2]

This paper examines the affinity of Cd^{2+} for commercially available carboxyl-terminated iron oxide beads (C-TIOB, Sigma) in aqueous electrolytes as a function of pH and [Cd^{2+}]. These particles can be regarded as model systems for certain kinds of soil, and their systematic study could provide much needed insight into the underlying physicochemical bases that govern adsorption and release of metal ions from such complex particulate media. The concentration of solution phase Cd^{2+} was measured using anodic stripping voltammetry (ASV) and the amount of adsorbed Cd^{2+} was calculated from the difference between ASV data collected before and after placing the particles in contact with the solution. Measurements were performed both as a function of [Cd^{2+}] in the μM range at constant pH (= 7), and of pH at constant [Cd^{2+}] (= 25 μM). The effect of dispersed particles on the ASV data was explored by taking advantage of the superparamagnetic character of C-TIOB, which allowed for the particles to be manipulated *within* the enclosed vessel, including confinement and removal, using an external magnet. Such unique magnetic properties have been ingeniously exploited by the groups of Willner, Vandegrift, and Heineman for electrocatalytic and immunoassay applications.[11−14]

Experimental Section

The concentration of Cd^{2+} both in the absence and in the presence of suspended or magnetically confined C-TIOB in the solution was measured by ASV using a glassy carbon (GC) rotating disk electrode (RDE, Pine Instruments, disk area: 0.164 cm^2) controlled by a Pine RDE 3 rotator. Potential control was achieved with a Potentiostat/Galvanostat (RDE3, Pine Instruments). Unless otherwise specified, all measurements were performed in 50 mL of N_2-purged, 10 mM 4-morpholinepropane sulfonic acid (MOPS, Fisher, 98%) buffer, in 0.1 M $NaClO_4$ (Aldrich, 99%) aqueous solutions prepared with ultrapure water (Millipore) containing $Cd(ClO_4)_2$ (Alfa, 99%) at a specified concentration. The solution pH, as measured with a Chemcadet pH meter, was adjusted by adding NaOH or $HClO_4$ at concentrations of 0.1 N for pH 4−6, and 1 N for pH 6−8. All values of [Cd^{2+}] reported herein were corrected for changes in the volume (less than ca. 5%) induced by such additions.

* To whom correspondence should be addressed.

10.1021/jp047360j CCC: $27.50
Published on Web 07/28/2004

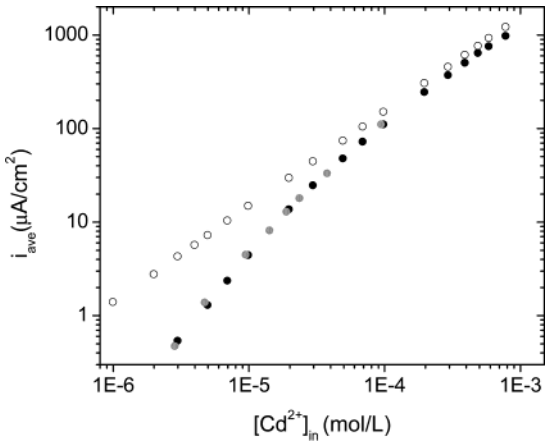

Figure 1. log−log plots of i_{ave} as a function of $[Cd^{2+}]_{in}$ recorded in the absence (○) and presence (black circle, gray circle) of 20 mg C-TIOB particles in 0.1 M $NaClO_4$ in 10 mM MOPS buffer solutions at pH = 7 (see text for details). The black and gray circles represent data obtained in two independent runs.

The metal deposition step was performed at a constant rotation rate, $\omega = 2500$ rpm, for 60 s, with the RDE polarized at −1.0 V vs SCE, a potential negative enough for Cd^{2+} deposition to proceed under strict diffusion limited control. The rotation was then interrupted, and the potential was immediately scanned at 5 mV/s in the positive direction up to 0.0 V vs SCE to strip the Cd metal deposits. Measurements of this type over a much wider $[Cd^{2+}]$ range were used to construct a calibration curve in the form of average deposition current, i_{ave}, i.e., integrated charge under the stripping peak divided by the total deposition time, i.e., 60 s, vs $[Cd^{2+}]$, yielding linear plots over the range 1 μM to 0.6 mM (see open circles in Figure 1).

Experiments involving Cd^{2+} adsorption were carried out by pipetting 1 mL of a C-TIOB suspension (Sigma, 240 μmol −COOH/g C-TIOB, 20 mg/mL in an aqueous suspension) under ultrasonic agitation. On this basis, this volume of suspension contains ca. 20 mg of particles which bear the equivalent of ca. 4.8 μmol −COOH. This aliquot was then placed in a cuvette and washed three times with pure water, using magnetic confinement (see below) and dispersion cycles, and then added as a wet powder to 50 mL of the buffer solution.

The extent of Cd^{2+} adsorption on C-TIOB (see below) as a function of $[Cd^{2+}]$ in the in μM range was determined at a single fixed pH (= 7) for a prescribed weight of particles in the solution, i.e., 20 mg, by adding small aliquots of $Cd(ClO_4)_2$ solutions, either 0.1 or 0.01 M, so as not to affect the volume significantly. No changes in the ASV were found in measurements recorded in sequence in the same solution affording strong evidence that steady-state adsorption is achieved very quickly.

The amount of Cd^{2+} adsorbed on the magnetic particles, $Q_{Cd^{2+}}$ in μmol Cd^{2+}/g C-TIOB was calculated from

$$Q_{Cd^{2+}} = V([Cd^{2+}]_{in} - [Cd^{2+}]_{fin})$$

where V is the volume of the solution, and $[Cd^{2+}]_{in}$ and $[Cd^{2+}]_{fin}$ represent the concentration of Cd^{2+} in the media, determined from the i_{ave} ASV values, using the calibration curves in Figure 1, before and after addition of C-TIOB to the medium, respectively.

Similar experiments were also carried out at a single $[Cd^{2+}]_{in}$ (= 25 μM) as a function of pH, both in ascending (pH 4 to 8.4) and descending order (pH 8.4 to 4).

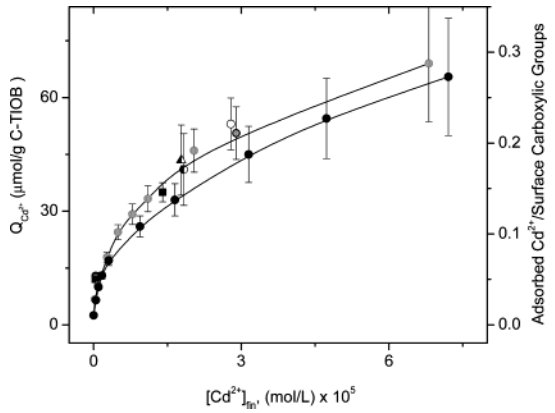

Figure 2. Plots of $Q_{Cd^{2+}}$ as a function of $[Cd^{2+}]_{fin}$ in 0.1 M $NaClO_4$ in 10 mM MOPS buffer solutions at pH = 7 in the presence of 20 mg C-TIOB. Also shown in this figure are the data in the form of the mole ratio of adsorbed Cd^{2+} to surface carboxylic groups (see right ordinate). The black and gray circles represent data obtained in two independent runs as indicated in Figure 1, and the lines through them are simple best fits (using splines) to these sets. Other symbols are explained in the text.

Analytical Considerations

Several factors can complicate the interpretation of ASV data recorded in the presence of C-TIOB in the solution under the conditions employed in this work:

i. Hydrodynamic flow distortions induced by the dispersed particles during the metal deposition step.

ii. Incorporation of particles into the metal deposits.

iii. Changes in the effective concentration of Cd^{2+} within the diffusion boundary layer of the RDE induced by dynamic equilibrium between Cd^{2+} adsorbed on the surface of the particles and in the solution phase, as thoroughly discussed in a more general context by van Leeuwen and co-workers.[15−17]

A series of experiments were designed to examine the extent to which these effects could affect the quantitative character of the data by taking advantage of the superparamagnetic properties of C-TIOB. First, ASV curves were recorded in 25 μM $[Cd^{2+}]$ in 10 mM MOPS/0.1M $NaClO_4$ buffered (pH = 7) solutions, both in the presence of 10 mg C-TIOB, and following their removal by filtration using a syringe-type arrangement (Disposable syringe filter, 0.45 μm Gelman Sciences). As evidenced by the results obtained, the ASV curves (not shown in this work) were virtually superimposable, yielding integrated values differing by no more than ca. 3%. The values of $Q_{Cd^{2+}}$ calculated from these data before (◐) and after (▲) filtration at ca. $[Cd^{2+}]_{fin}$ = 18.3 μM are shown in Figure 2. A discussion of error propagation will follow later in this section.

A variant of the experiment above was devised in which an external permanent magnet (NdFeB, Edmund Industrial Optics) was used to confine the particles *in* the solution and a new ASV recorded. The results obtained for 5 and 50 μM Cd^{2+} solutions for 20 mg C-TIOB dispersed (D) and subsequently magnetically confined *in* the solution (MCi) are shown in the form of histograms in panels A and B in Figure 3, as either i_{ave} (left ordinate) or i_{ave} normalized by the value recorded before adding particles to the solution shown as bar F in this figure (see right ordinate). The confined particles were then removed from the solution by displacing the magnet along the walls of the vessel and new ASV data collected and analyzed yielding the value displayed as MCo in the histogram. The overall procedure was then reversed by first bringing the confined particles into the solution (rMCi) and finally allowing them to redispersed by removing the magnet altogether (rD). As indicated in Figure 3,

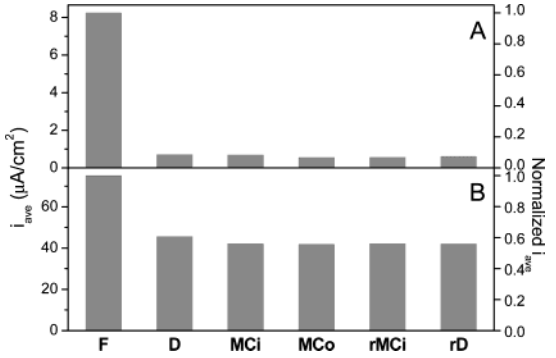

Figure 3. Histograms of i_{ave} for 5 (panel A) and 50 μM (panel B) Cd^{2+} in 0.1 M $NaClO_4$ in 10 mM MOPS buffer solutions at pH = 7 before (F) and after adding 20 mg of C-TIOB into the solution, for the particles dispersed (D), magnetically confined in the solution (MCi), removed from the solution, by displacing the magnet along the walls of the vessel (MCo), reintroduced into the solution (rMCi) and finally redispersed by removing the magnet (rD). The right ordinate represents the same data normalized by i_{ave} before adding 20 mg C-TIOB particles into the solution (F).

i_{ave} was larger when the particles were dispersed in (see D and rD, in Figure 3) than when removed magnetically from the solution (see MCo in the same figure). The average values of $Q_{Cd^{2+}}$ in the presence of particles (see the gray circle outlined in black in Figure 2), based on D and rD in Figure 3, were larger than those obtained from measurements in which the C-TIOB were confined outside the solution (see ○ in Figure 2) by 1.3% and 6.1% for $[Cd^{2+}]_{in} = 5$ and 50μM, respectively.

The relative error in $Q_{Cd^{2+}}/V = \alpha(\{[Cd^{2+}]_{in}^2 + [Cd^{2+}]_{fin}^2\}^{1/2})/([Cd^{2+}]_{in} - [Cd^{2+}]_{fin})$ increases with Cd^{2+} concentration, where α is the (fixed) relative error in the concentration measurement. Assuming $\alpha = 5\%$, the relative error in $Q_{Cd^{2+}}/V$ for $[Cd^{2+}]_{in} = 50$ μM is 18.8% and thus much larger than that caused by the larger i_{ave} in the presence of the particles in the solution, i.e., 6.1%, as discussed above.

In summary, ASV affords a versatile in situ means of determining reliable values of the extent of Cd^{2+} adsorption on dispersed C-TIOB. As will be shown in the next section, this method can be conveniently used to establish correlations between the amount of Cd^{2+} adsorbed on C-TIOB and $[Cd^{2+}]_{fin}$, elucidating the various factors that govern the interactions between the metal ion and the functionalized nanoparticles, including adsorption isotherms and the effect of pH.

Results and Discussion

a. Effects of $[Cd^{2+}]$. Shown in Figure 1 is a log−log plot of i_{ave} as a function of $[Cd^{2+}]_{in}$ up to 0.1 mM before (open circles) and after (solid circles) dispersing 20 mg C-TIOB in the solution, where the black and gray circles represent data obtained in two independent runs. As indicated, i_{ave} decreased upon addition of particles to the solution in the entire range of $[Cd^{2+}]$ examined. This behavior is consistent with Cd^{2+} adsorption on carboxylic groups on C-TIOB and in line with that observations made on flat surfaces[8,18] and other particulate media reported elsewhere.[19,20] These results can be displayed in a more useful form in terms of $Q_{Cd^{2+}}$ in μmol Cd^{2+}/g C-TIOB (see left ordinate, Figure 2), or alternatively in terms of mole ratio of adsorbed Cd^{2+} to surface carboxylate/carboxylic groups (see right ordinate in the same figure) as a function of $[Cd^{2+}]_{fin}$ for $[Cd^{2+}]_{in}$ up to 70 μM (see the black and gray circles in this figure). At higher concentration, the error becomes very large (>20%) and therefore no data are given. It is interesting to note that the values on the right ordinate in Figure 2 are still below 0.5, which corresponds formally to full electroneutrality, i.e., 1 Cd^{2+} per 2 ($-COO^-$).

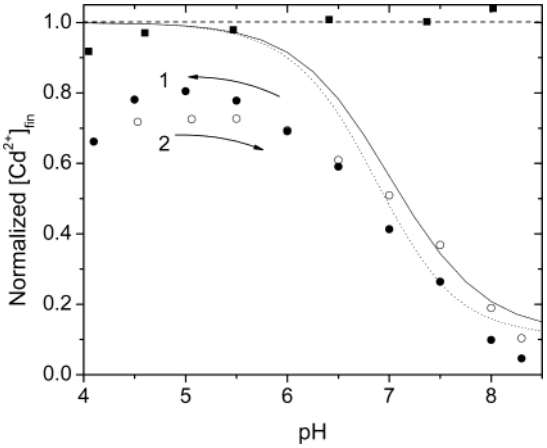

Figure 4. Plots of normalized $[Cd^{2+}]_{fin}$ in solution as a function of pH for 25 μM $Cd(ClO_4)_2$ in 0.1 M $NaClO_4$/10 mM MOPS solutions in the absence (solid squares) and the presence of 20 mg of C-TIOB recorded for decreasing (solid circles) starting at pH 8.3 and subsequently for increasing pH (open circles). The solid line in this figure was obtained from a simulation involving solution phase species (no particles) containing 96 μF (micro formal) of a carboxylic acid with $pK_a = 8.00$, and a metal-carboxylate binding constant of 10^5. The dotted line in this figure represents the results of yet another simulation for a solution containing the same amount of Cd^{2+} and a concentration of acetate of ca. 96 mF (see text for details).

In additional experiments, adsorbed Cd^{2+} on C-TIOB in equilibrium with $[Cd^{2+}]_{fin}$ either 0.48 or 30.1 μM (see the gray circle outlined in black in Figure 2) was confined *in* the solution with the external magnet, and the liquid was removed with a syringe. Subsequently, fresh buffer *without* Cd^{2+} was added to the vessel and ASV was recorded within several hours, while the particles were kept magnetically confined *in* the solution. As evidenced from the data (not shown here), the amount of Cd^{2+} detected even for the more concentrated solution was very small. However, upon removing the magnet to allow full particle dispersion, the resulting ASV yielded values of $[Cd^{2+}]_{fin}$ of 0.34 and 14 μM (see ■ in Figure 2), respectively. As shown in the figure, these new points lie very close to the original adsorption curve; hence, to a good degree of approximation and within the concentration range examined, the adsorption process is reversible, and therefore, the data represents the adsorption isotherm. Unfortunately, the data appears too limited and the errors involved in the high concentration region are too large to warrant further analysis of the functional form of the adsorption isotherm. Other methods capable of measuring directly the amount of adsorbed metal would be required to provide more reliable values over a more extended concentration range.

b. Effect of Solution pH. A series of experiments were performed with $[Cd^{2+}]_{in} = 25$ μM in 10 mM MOPS in 0.1 M $NaClO_4$ (Aldrich, 99%) buffer solutions, both in the absence and presence of 20 mg of C-TIOB in the media, to determine changes in $[Cd^{2+}]$ (or, equivalently, in the amount of Cd^{2+} uptake) as a function of pH. As shown in solid squares in Figure 4, the values of $[Cd^{2+}]$ derived from i_{ave} in the range $4 < pH < 8.5$, in the absence of C-TIOB, normalized by the average of the six data points, $[Cd^{2+}]_{ave}$, were found to be fairly independent of pH. Corresponding values for $[Cd^{2+}]_{fin}$ determined in the presence of dispersed C-TIOB normalized by $[Cd^{2+}]_{ave}$ (open and solid circles in Figure 4) were much lower, i.e., >20% over the entire pH region, consistent with the binding of Cd^{2+} to the particles. As indicated, the normalized $[Cd^{2+}]$

data collected first in descending (filled circles) starting at pH 8.3, and then in ascending (see open circles) pH, yielded in this case a plateau for 4.1 < pH < ca. 5.5, followed by a steady decrease as the pH increased. Also noteworthy is the fact that the values observed were fairly independent of whether the pH was increased or decreased. However, excursions to much lower pH values, e.g., 3, led to a loss of adsorption efficiency (not shown in this figure), probably caused by the onset of dissolution of hematite (and thus of surfactant) into the media.

This overall behavior can be rationalized, at least, qualitatively based on solution phase equilibria, by assuming pK_a (for the surface carboxylic acid) of ca. 8, and a metal-carboxylate complexation constant of 10^5 (see solid line in Figure 4). Both of these values are ca. 3 units higher than those reported for free carboxylic monoacids, and also for the Cd^{2+} acetate complex in solution phase.[21] Such an upward shift in pK_a has been well documented for alkane-type SAM bearing carboxylic groups (and other surfaces as well),[9,22] and attributed, at least in part, to the increased proton affinity of the ensemble of closely packed negatively charged carboxylate groups.[22,23] Based on these considerations, the same effect would be expected to occur for metal ion binding, as evidenced by the much lower value of the complexation constant of Cd^{2+} with acetate (1.61 and 1.07) compared to oxalate (3.71).[21]

The results of the simulation point to extraordinary enhancements in the affinity of carboxylate for Cd^{2+} (and numerous other metal ions as well) induced by surface immobilization at the high coverage levels involved in C-TIOB. This effect is best illustrated by calculating the extent of complexation in homogeneous solutions containing carboxylate/carboxylic groups at the same equivalent concentration as that used in the experiments, i.e., 20 mg C-TIOB x 240 nmol $COOH/COO^-$ per mg, or 4.8×10^{-6} mol/0.05 L = 96 μF (microformal), and the same concentration of cadmium, i.e., 25 μF. Based on simple solution phase equilibrium calculations (see Supporting Information), hardly any Cd^{2+} (<0.5%) will be complexed by carboxylate for solutions 4 < pH < 9. In fact, to promote binding to the level found for the carboxyl-bearing particles, the concentration of $COOH/COO^-$ groups in the solution would have to be raised by at least 3 orders of magnitude (see dotted line in Figure 4).

One possible explanation for the lower (normalized) $[Cd^{2+}]_{fin}$ measured in the plateau region (blank circles), i.e., ca. 20%, compared to solutions devoid of particles (see solid squares in Figure 4), may be found in the presence of specific sites on the surface displaying high affinity for Cd^{2+}, which become saturated in the entire pH region examined for $[Cd^{2+}]$ at which these experiments were performed. Some evidence in support of this view has been provided by Scoles et al., who studied Cd^{2+} adsorption on SAMs bearing carboxylic terminal groups supported on Au,[20] where adsorption of the metal ion was either found to be irreversible, or showed large hysteresis when the pH value was decreased. In fact, in their studies, the presence of adsorbed Cd^{2+} on SAM could be verified from ex situ X-ray measurements of films removed from the solution and could only be eliminated by washing with a 0.01 M solution of HNO_3.

Concluding Remarks

The most salient aspects of the work herein described may be summarized as follows:

1. Confinement of carboxylic/carboxylate groups at rather high coverages, i.e., ca. 0.1 nmol/cm^2, to surfaces of the type examined in this work, promotes the reversible binding of solution phase Cd^{2+} in aqueous electrolytes. This phenomenon is conceptually analogous to the upward shift in pK_a for carboxyl terminated surfaces, compared to those found in solution phase, and thus consistent with an increase in the *effective* metal−ligand complexation constant for the heterogeneous system.

2. Within the limitations specified above, in situ ASV may be regarded as being sensitive only to solution phase species and, thus, offers a number of advantages over alternate ex situ techniques reported in the literature.

Supporting Information Available: Simple solution phase equilibrium calculations. This material is available free of charge via the Internet at http://pubs.acs.org.

References and Notes

(1) Zalups, R. K.; Ahmad, S. *Toxicol. Appl. Pharmacol.* **2003**, *186*, 163−188.
(2) Bolton, K. A.; Evans, L. J. *Can. J. Soil Sci.* **1996**, *76*, 183−189.
(3) Nriagu, J. O.; Pacyna, J. M. *Nature* **1988**, *333*, 134−139.
(4) Tajmirriahi, H. A.; Ahmed, A. *J. Mol. Struct.* **1993**, *297*, 103−108.
(5) Ahmed, A.; Tajmirriahi, H. A. *J. Inorg. Biochem.* **1993**, *50*, 235−243.
(6) Trivedi, P.; Axe, L. *Environ. Sci. Technol.* **2000**, *34*, 2215−2223.
(7) Petrovic, M.; Kastelan-Macan, M.; Horvat, A. J. M. *Water Air Soil Pollut.* **1999**, *111*, 41−56.
(8) Stefan, I. C.; Mandler, D.; Scherson, D. A. *Langmuir* **2002**, *18*, 6976−6980.
(9) Stefan, I. C.; Scherson, D. A. *Langmuir* **2000**, *16*, 5945−5948.
(10) Burshtain, D.; Wu, J.; Melman, A.; Mandler, D.; Scherson, D. A. *Langmuir* **2004**, *20*, 4498−4502.
(11) Katz, E.; Sheeney-Haj-Ichia, L.; Willner, I. *Chem.-Eur. J.* **2002**, *8*, 4138−4148.
(12) Nunez, L.; Buchholz, B. A.; Kaminski, M.; Aase, S. B.; Brown, N. R.; Vandegrift, G. F. *Sep. Sci. Technol.* **1996**, *31*, 1393−1407.
(13) Nunez, L.; Buchholz, B. A.; Vandegrift, G. F. *Sep. Sci. Technol.* **1995**, *30*, 1455−1471.
(14) Wijayawardhana, C. A.; Purushothama, S.; Cousino, M. A.; Halsall, H. B.; Heineman, W. R. *J. Electroanal. Chem.* **1999**, *468*, 2−8.
(15) Wonders, J.; vanLeeuwen, H. P. *J. Electroanal. Chem.* **1996**, *401*, 103−112.
(16) Wonders, J.; Van Leeuwen, H. P. *Electrochim. Acta* **1998**, *43*, 3401−3412.
(17) DiazCruz, J. M.; Wonders, J.; vanLeeuwen, H. P. *Electroanalysis* **1995**, *7*, 1143−1150.
(18) Turyan, I.; Mandler, D. *Anal. Chem.* **1994**, *66*, 58−63.
(19) Hong, A. P. K.; Chen, T. C. *Water Air Soil Pollut.* **1996**, *86*, 335−346.
(20) Li, J.; Liang, K. S.; Scoles, G.; Ulman, A. *Langmuir* **1995**, *11*, 4418−4427.
(21) Sillen, L. G.; Martell, A. E. *Stability Constants of Metal-Ion Complexes, Supplement No. 1, Pts. 1 and 2: Inorganic Ligands. Organic Including Macromolecule Ligands*; Chemical Society, Special Publication No. 25, 1971.
(22) Kakiuchi, T.; Iida, M.; Imabayashi, S.; Niki, K. *Langmuir* **2000**, *16*, 5397−5401.
(23) Creager, S. E.; Clarke, J. *Langmuir* **1994**, *10*, 3675−3683.